Applied Microbiology and Biotechnology (2024) 108:496
https://doi.org/10.1007/s00253-024-13336-7



# Heterologous expressing melittin in a probiotic yeast to evaluate its function for promoting NSC-34 regeneration

**Hsiao-Yun Huang[1] · Hung-Yi Hsu[2,3] · Cheng-Yu Kuo[4] · Mao-Lun Wu[1] · Chien-Chen Lai[4] · Gary Ro-Lin Chang[1] · Yu-Ju Lin[1]**

Received: 21 March 2024 / Revised: 21 September 2024 / Accepted: 16 October 2024 / Published online: 28 October 2024


## Abstract

Melittin is a bioactive peptide and the predominant component in bee venom (BV), studied for its many medical properties, such as antibacterial, anti-inflammatory, anti-arthritis, nerve damage reduction, and muscle cell regeneration. Melittin is primarily obtained through natural extraction and chemical synthesis; however, both methods have limitations and cannot be used for mass production. This study established a heterologous melittin expression system in the probiotic yeast *Kluyveromyces marxianus*. This yeast was selected for its advantages in stress tolerance and high secreted protein yields, simplifying purification. A > 95% high-purity melittin (MET) and its precursor promelittin (ProMET) were successfully produced and purified at 1.68 μg/mL and 3.33 μg/mL concentrations and verified through HPLC and mass spectrum. The functional test of the NSC-34 cell regeneration revealed that MET achieved the best activity compared to ProMET and the natural-extracted BV groups. Growth-related gene expressions were evaluated, including microtubule-associated protein 2 (*MAP2*), microtubule-associated protein Tau (*MAPT*), growth-associated protein 43 (*GAP-43*), choline acetyltransferase (*ChAT*), vesicular acetylcholine transporter (*VAChT*), and acetylcholine esterase (*AChE*). The results indicated that treating MET increased *MAP2*, *GAP-43*, and *VAChT* expressions, in which cholinergic signaling is related to neurological functions. A heterologously expressed melittin in a probiotic yeast and its potential for promoting NSC-34 regeneration described here facilitate commercial and therapeutic use.

### Key points

- *MET and its precursor ProMET were successfully hetero-expressed in K. marxianus*
- *> 95% high-purity MET and ProMET were purified at 1.68 μg/mL and 3.33 μg/mL*
- *MET has no cytotoxicity toward NSC-34 and significantly promotes NSC-34 growth*

**Keywords** Melittin · *Kluyveromyces marxianus* · Bee venom · Heterologous expression system · NSC-34 motor neurons · Cell growth–related factor gene expression

## Introduction

Bee venom (BV) is a complex mixture of natural products from the honey bee (*Apis mellifera*), containing various substances employing pharmaceutical properties, such as peptides, enzymes, biologically active amines, and non-peptide components. Since BV therapy has been applied to acute and chronic human diseases, more interests focus on its anti-neurodegeneration ability (Hwang et al. 2015). However, allergens must be effectively removed and integral components isolated to protect patients against potential BV extraction side effects. Melittin is the most abundant BV component, which is a peptide comprising 50–60% of the dry weight (DW) (Abd El-Wahed et al. 2019; Pacakova et al. 1995; Pucca et al. 2019). Moreover, melittin exhibits various biological activities with remarkable clinical and therapeutic effects (Carpena et al. 2020). Melittin is a cationic, linear α-helical polypeptide formed by 26 amino acid (AA) residues, soluble in water, and amphipathic and maintains a 2846.5 Da molecular weight. In addition, melittin has a hydrophobic N-terminus and a hydrophilic C-terminus suggesting to be the bioactive peptides ability (Wang et al. 2009). A previous study has demonstrated that melittin

Hsiao-Yun Huang and Hung-Yi Hsu contributed equally to this work.

Extended author information available on the last page of the article

exhibits neuroprotective actions via reducing proinflammatory mediators in lipopolysaccharide-stimulated BV2 microglia (Moon et al. 2007) and protects neuroblastoma SH-SY5Y cells against $H_2O_2$-induced neurotoxicity (Han et al. 2014).

Melittin displays low molecular weights and is an amphiphilic structure with potential medicine and agriculture value, but the amount and purity limit its applications. There are three methods for melittin preparation: extraction from natural BV, chemical synthesis, and biological preparation (Lee et al. 2018). However, natural extraction's safety and ecological effects are prominent concerns, while chemical synthesis is expensive and raises environmental pollution issues, inhibiting mass production. Many studies on preparing active peptides through biological methods report considerable development prospects. These techniques still present significant challenges. For example, heterologous production of melittin in *Escherichia coli* was previously established (Chen et al. 2021; Zhou et al. 2020) but worries for the host remained, such as safety limits concerning its downstream application for human consumption. Moridi et al. expressed melittin in *Pichia pastoris*, but the 0.105 µg/mL production following partial purification was low (Moridi et al. 2020) because of its high toxicity and small molecular weight. Although Husseneder et al. (2016) successfully produced melittin using *Kluyveromyces lactis*, biological assays were limited in scope (Husseneder et al. 2016). Thus, it is still a problem to industrialize applications of melittin.

Heterologous melittin expression is also challenging due to its high toxicity against a broad microorganism range (Muñoz et al. 2007; Portell-Buj et al. 2019). Therefore, this study used the probiotic yeast *K. marxianus* to establish a probiotic therapy platform for producing biologically active melittin. *K. marxianus* has several advantages, including a thermos and toxin tolerance, high secretory capacity, and relatively low protease types regarding heterologous protein degradation (Fonseca et al. 2008). As such, *K. marxianus* is a promising drug delivery carrier for therapeutic applications (Hong et al. 2007). This study proposes a sustainable method for manufacturing melittin in the probiotic yeast *K. marxianus* as a probiotic venom therapy. A previous study has shown that melittin can enhance muscle regeneration factors expression (Lee et al. 2019). To explore the medical abilities of melittin preparation by heterologous expression, this study also tested its functions of cell regeneration and the protection of neuronal cells in oxidative stress.

## Materials and methods

### Construction and transformation of MET-expressed cassettes

*MET* and precursor *ProMET* genes from *Apis mellifera* were codon-optimized toward *K. marxianus* and synthesized (Twist Bioscience, USA), which sequences are shown in Fig. S1. Sequence design and optimization for the two constructions (pKLAC2-a-his-MET and pKLAC2-a-his-ProMET) were inserted in a plasmid (pKLAC2-a-) between *Nde*I and *Not*I restriction enzyme sites. *K. marxianus* BCRC 22057 was transformed with *Sac*II-linearized plasmids and integrated into the *lac4* promoter (Fig. 1A), following a previously reported protocol (Lin et al. 2017). The peptide expression of melittin in this study was named MET and promelittin was ProMET.

Transformants were screened in a YPG medium supplemental with G418 (200 µg/mL, Sigma, USA), and the wild type was used as a control. Successfully engineered colonies were validated through PCR amplification of the integrated genes, using yeast colony DNA as a template with the universal S1274F, S1276R, and gene-specific primer

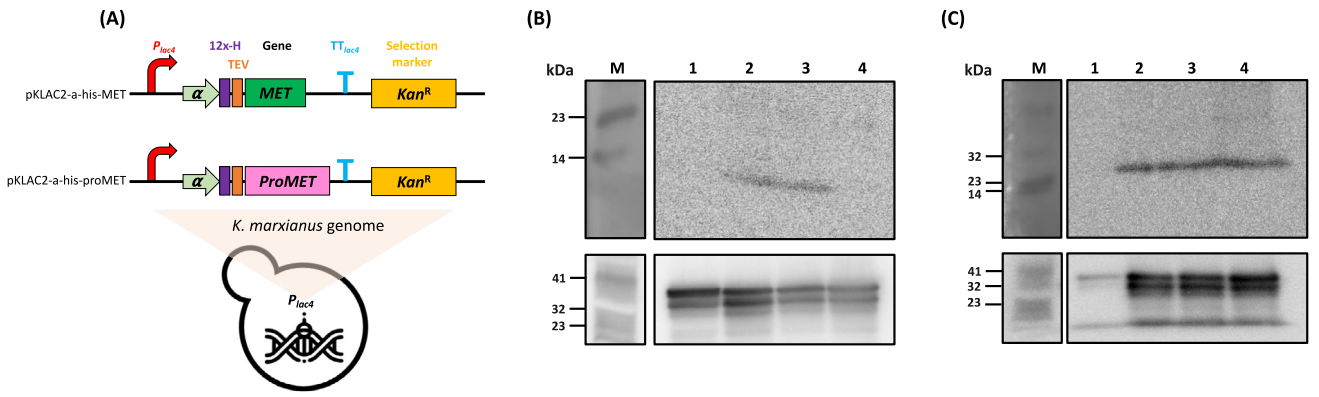


**Fig. 1** MET and ProMET construction and Western blotting assays in a yeast culture supernatant. **A** Schematic representation of *K. marxianus*e expressing *MET* and *ProMET*; **B** Western blotting analysis of MET; **C** Western blotting analysis of ProMET. Lane 1, day 1; lane 2, day 2; lane 3, day 3; lane 4, day 4

pairs. Yeast colony DNA was obtained through treatment with the QuickExtract DNA Extraction Solution (Lucigen, USA). Subsequently, gene stability was confirmed after three generations to obtain the stable strain.

## Western blotting

Western blotting analysis was performed following the previous study with modifications to evaluate MET and ProMET production (Lee et al. 2020). Briefly, 10 mL of the yeast supernatant was harvested after culturing in YPG for 1 to 4 days, and total proteins were precipitated by adding an equal volume of 20% trichloroacetic acid (Acros Organics, Belgium) on ice for 30 min. After centrifugation at 13,200 rpm for 15 min at 4 °C, 300 µL cold acetone (Macron Fine Chemicals, USA) was added, and this step was repeated thrice. The protein sample was dried and dissolved in 50 µL LDS sample buffer (M00676-250, GenScript, USA), which was loaded onto Tris–glycine SDS–polyacrylamide gel electrophoresis (SDS-PAGE, SurePAGE™ 4–12% BT, GenScript, USA) and run through electrophoresis with the Tris-MOPS-SDS running buffer (GenScript, USA). Following electrophoresis, the SDS-PAGE was transferred to the 100% methanol-activated FluoroTrans® W3.3 PVDF transfer membrane (Pall Corporation, USA) by the Western blot transfer system (GenScript/eBlot L1, USA). The PVDF membrane was blocked in 5% skim milk (Sigma, USA) at RT for 2 h and incubated with HRP-conjugated 6×His antibody (Mouse McAb, ProteinTech, USA) at RT for 1 h to detect MET or incubated with GAPDH antibody (Rabbit Ab, GeneTex, USA) as an internal control. Lastly, the membrane was shaken and washed with phosphate-buffered saline with Tween 20 (PBST) at RT and imaged for detecting protein on an ImageQuant LAS 4000 system (General Electric, USA) with ECL™ Western blotting detection reagents (Amersham, UK).

## Histidine affinity chromatography

The successful yeast transformant was cultured in 5 mL YPG medium supplemental with G418 (200 µg/mL) and sub-cultured to 100 mL YPG. After culturing for 2 days at 30 °C, the yeast supernatant was harvested and passed through gravity-flow columns (Bio-Rad, USA) packed by 600 µL nickel (Ni) beads (Thermo Scientific, USA) and reached equilibrium with 6 mL buffer A (50 mM Tris, 150 mM NaCl, 20 mM imidazole, pH 8.0). The sample was washed with 240 mL buffer A and eluted with 2.4 mL buffer B (50 mM Tris, 150 mM NaCl, 250 mM imidazole, pH 8.0). The purified sample was evaluated by SDS-PAGE and Western blotting.

## Dialysis

First, 5 mL of purified sample was loaded onto Float-A-Lyzer G2 (Spectrum Laboratories Inc., USA) equipment, the floated dialysate of 1X PBS buffer was stirred at 125 rpm, and the dialysate was replaced after 2–4, 6–8, and 10–14 h. The dialyzed sample was collected after dialysis.

## TEV protease treatment and desalting

The 5 mL dialyzed sample was treated with five units of TEV protease (T4455, Sigma-Aldrich, USA) and shaken at 70 rpm for 1 h at 30 °C to cleave the N-terminal histidine tag. After TEV protease treatment, the sample was purified by nickel (Ni) beads, as previously described, to remove TEV protease and collect the flow-through sample. The sample was desalted through a Sephadex G-25 Coarse PD-10 Desalting column (Cytiva, USA) and eluted by $ddH_2O$ to obtain purified MET and ProMET. The protein concentration was quantified with the Pierce™ Detergent Compatible Bradford Assay Kit (Bio-Rad, USA).

## HPLC

The following samples were prepared and qualified through HPLC: (1) $ddH_2O$, the control; (2) BV-A4-1, natural crude BV extract (kindly provided by Dr. Ming-Cheng Wu, Chung Hsing University, Department of Entomology); (3) BV-CITEQ (19C10, Citeq Biologics, Netherlands), commercial crude BV extract; (4) MET, purified MET from this study; (5) ProMET, purified ProMET from this study; and (6) MET-no TEV, TEV protease untreated MET. Samples were centrifuged for 5 min at 10,000 rpm to remove particles. Then, the supernatant was separated by a TSKgel G2000SWXL column (Tosoh Bioscience GmbH, Germany), and the SAPPHIRE 800 UV–VIS Variable Wavelength DETECTOR (Czechia) detected absorbance under 215 nm. HPLC was operated at 25 °C and a 0.5 mL/min flow rate with a 0.1 M potassium phosphate and 1 M NaCl (pH 6.5) mobile phase for 50 min. Data was analyzed by PEAK-ABC software.

## Mass spectrum

The purified samples of MET and ProMET were first desalted using C18 ZipTip and resuspended in 0.1% formic acid (FA). They were then analyzed by ultra-performance liquid chromatography (UPLC, Dionex Ultimate 3000, Thermo Fisher Scientific) coupled with a quadrupole-time-of-flight mass spectrometer (Q-TOF MS, triple 6600, SCIEX). A C18 column (bioZen 2.6 µm Peptide XB-C18, Nano Column, 250×0.075 mm, Phenomenex) was used to separate the peptides, with 0.1% FA in $DIH_2O$ and 0.1% FA

in acetonitrile selected as mobile phases A and B, respectively. The gradient was set as follows: 0–4.5 min, 5% B; 4.5–31 min, 5–35% B; 31–32 min, 35–90% B; 32–52 min, 90% B, 52–53 min, 90–5% B; and 53–70 min, 5% B. The scan mode was configured for data-dependent acquisition (DDA) with a scan range of 350–2000 m/z and 50–1900 m/z for MS1 and MS2, respectively. The MS data were analyzed by Mascot software with the database of MET and ProMET sequences.

### Establishment of NSC-34 cell standard curve

The NSC-34 cell was produced by fusing neuroblastoma and motor neurons (kindly provided by Dr. Pei-Chien Tsai, National Chung Hsing University, Department of Life Sciences). Cells were harvested after 3 days of activation and resuspended in DMEM medium (Dulbecco's Modified Eagle Medium, Thermo, USA) containing 10% FBS (Fetal Bovine Serum, Thermo, USA), 100 U/mL penicillin, and 100 µg/mL streptomycin. After counting the cells, 100 µL of $6.25\times10^2$, $1.25\times10^3$, $2.5\times10^3$, $2\times10^4$, and $4\times10^4$ cells were inoculated into a 96-well cell culture dish (Nunc™ MicroWell™ 96-Well, Thermo, USA), and 10 µL Cell Counting Kit-8 (CCK-8, TargetMol, USA) was added to measure cell viability. The plates were cultured at 37 °C with 5% $CO_2$ for 1–4 h until the color turned orange. The PARADIGMTM Selection Platform system (Beckman Coulter, USA) detected each plate's value at a 450 nm absorbance value (Bio-Rad, Hercules, CA, USA). Cell numbers and absorbance values were taken to establish a standard calibration line and calculate the actual cell number in cell growth rate and regeneration experiments.

### Evaluation of the NSC-34 growth rate

This experiment was modified based on that of Jung et al. (Jung et al. 2015). Cells were harvested after 3 days of activation and resuspened in DMEM (Dulbecco's Modified Eagle Medium, Thermo, USA) containing 10% FBS (Fetal Bovine Serum, Thermo, USA), 100 U/mL penicillin, and 100 µg/mL streptomycin. After counting the cells, 100 µL of $2\times10^4$ NSC-34 cells was inoculated into a 96-well cell culture dish (Nunc™ MicroWell™ 96-Well, Thermo, USA) and cultured at 37 °C with 5% $CO_2$ for 1 day. Fifty microliters of test samples was treated on cells with triplicate, including the following: (1) $ddH_2O$, the control; (2) BV-A4-1, natural crude BV extract (kindly provided by Dr. Ming-Cheng Wu, Chung Hsing University, Department of Entomology); (3) BV-CITEQ (19C10, Citeq Biologics, Netherlands), commercial crude BV extract; (4) M, purified MET from this study; and (5) P, purified ProMET from this study. After treatment, cells remained in culture at 37 °C with 5% $CO_2$ for 0, 6, 12, and 24 h. Next, 15 µL of Cell Counting Kit-8 (CCK-8, TargetMol, USA) was added into each group at each time point to measure cell viability and incubated at 37 °C with 5% $CO_2$ for 1–4 h. When the color turned orange, each plate was shaken for 1 min, and the PARADIGMTM Selection Platform system (Beckman Coulter, USA) was used to detect values at 450 nm absorbance (Bio-Rad, Hercules, CA, USA). The cell growth rate was calculated using the formula: 100% + ((time point − 0 h baseline)/0 h baseline) × 100%.

### NSC-34 regeneration after $H_2O_2$ damage

This experiment was modified based on studies by Jung et al. (Jung et al. 2015) and Maier et al. (Maier et al. 2013). One hundred microliters of activated $2\times10^4$ NSC-34 cells were inoculated into a 96-well cell culture dish (Nunc™ MicroWell™ 96-Well, Thermo, USA) and cultured at 37 °C with 5% $CO_2$ for 1 day. $H_2O_2$ was added to a final 50 µM concentration, where $ddH_2O$ was added as the non-$H_2O_2$-damaged control group (control) and incubated at 37 °C with 5% $CO_2$ for 1 day. Fifty microliters of test samples was treated in triplicate, including the following treatment groups: (1) BV-A4-1, natural crude BV extract (kindly provided from Dr. Ming-Cheng Wu, Chung Hsing University, Department of Entomology); (2) BV-CITEQ (19C10, Citeq Biologics, Netherlands), commercial crude BV extract; (3) M, purified MET from this study; and (4) P, purified ProMET from this study. The cell viability was measured by Cell Counting Kit-8 (CCK-8, TargetMol, USA) as previously described. Cell regeneration fold change was calculated with the formula: treatment (time point − 0 h baseline)/control (time point − 0 h baseline).

### Gene expression

RNA was extracted with the NucleoSpin RNA kit (Macheret-Nagel, Germany). Briefly, 1 mL of $2\times10^5$ NSC-34 was inoculated into a 3.5-mm culture dish (Thermo, USA), cultured at 37 °C with 5% $CO_2$ for 1 day, and then treated with 500 µL of test samples for 24 h as previously described. After pouring off the medium, 350 µL buffer RA1 and 3.5 µL β-mercaptoethanol were added and scraped off the attached cells. The total cell solution was added to the NucleoSpin® Filter and purified with the NucleoSpin® RNA kit manual. The extracted RNA's concentration and quality were measured by a Nano-100 full-wavelength micro-spectrophotometer (CLUBIO, Taiwan) and stored at − 80 °C.

cDNA synthesis was prepared with the SuperScriptTM IV First-Strand Synthesis System Kit (Thermo, USA). One microliter of 50 µM Oligo d(T)20 primer, 1 µL 10 mM dNTP mix, 4 µL 1 µg Template RNA, and 7 µL DEPC-treated water (a total volume of 13 µL) were mixed and maintained at 65 °C for 15 min in the PCR machine (SensoQuest,

model: Labcycler Gradient, Germany) for first-strand cDNA synthesis. The RT reaction mixture, including 4 µL 5X SSIV Buffer, 1 µL 100 mM DTT, 1 µL ribonuclease inhibitor, 1 µL SuperScript™ IV reverse transcriptase (200 U/µL), and first-strand cDNA, was added (a total volume of 20 µL) and reacted at 55 °C for 30 min and at 80 °C for 10 min. Then, 1 µL of *E. coli* RNase H (2 U/µL) was added to react at 37 °C for 20 min.

The significantly expressed genes from a different treatment were assessed through qPCR. Briefly, the qPCR reaction solution was mixed as follows: 10 µL 2X iQ™ SYBR® Green Supermix (Bio-Rad, USA), 1 µL 10 µM cell growth gene marker primer pairs (Maier et al. 2013) (Table 1), 4 µL sterile water, and 4 µL of the previously prepared 50 ng/µL cDNA template. qPCR was performed by the qPCR Biometra/846–070-000 (Germany) program at 95 °C for 10 min, 95 °C for 15 s, and 60 °C for 1 min as one cycle. The real-time quantitative PCR reaction was conducted for 45 cycles. The expression level was calculated with the formula: $2^{-(\Delta\Delta Ct)}$. $\Delta\Delta Ct = (\Delta Ct \text{ treated}) - (\Delta Ct \text{ untreated})$; $\Delta Ct = (\text{sample average Ct}) - (\beta\text{-actin Ct})$.

## Data analysis

The experimental and control groups differed significantly regarding cell viability and gene expression results. The groups were compared using a one-way analysis of variance (ANOVA) and the least-significant difference test in SPSS version 25.0 (IBM, Armonk NY, USA). $p$ values of $< 0.05$ were considered significant.

**Table 1** Primers used for growth-related gene expressions

| Name | Primers (5′→3′) | Product size (bp) |
|---|---|---|
| MAP2 | F: TGCCACCTGTTTCTCTCCAC<br>R: TCTTTTGCTTGCTCGGGATT | 193 |
| MAPT | F: AAGGGGTATTGGGCAGAAGG<br>R: CTTTTCCTGTGGGAGCGAAG | 161 |
| GAP-43 | F: TAAGGAAAGTGCCCGACAGG<br>R: TGAGCAGGACAGGAGAGGAAA | 160 |
| ChAT | F: CCAACCAAGCCAAGCAATCT<br>R: AAGGATAGGGGAGCAGCAACAA | 114 |
| VAChT | F: GCGATGTGCTGCTTGATGA<br>R: TTGACCTAAATGGGGAGGGTA | 196 |
| AChE | F: ACCTTCCCTGGCTTTTCCAC<br>R: GCATCCAACACTCCTGACCA | 248 |
| β-actin | F: CCAGCCTTCCTTGGGTAT<br>R: TGCTGCTGGAAGGTGGACAGTGAG | 297 |

*MAP2: microtubule-associated protein 2, MAPT: microtubule-associated protein Tau, GAP-43: growth-associated protein 43, ChAT: choline acetyltransferase, VAChT: vesicular acetylcholine transporter, and AChE: acetylcholine esterase

# Results

## MET and ProMET in *K. marxianus* construction and expression

Melittin and promelittin cDNA were expressed using the inducible promoter *lac4,* and its expression profile was studied by culture in 2% galactose. Two expression plasmids, pKLAC2-a-his-MET and pKLAC2-a-his-ProMET, were constructed, *Sac*II-linearized, and integrated into the *K. marxianus* genome (Fig. 1A). Heterologous gene stability was tested for three generations by randomly selecting five sub-cultured colonies (Fig. S2).

Strains stably expressing melittin and promelittin were selected and cultured for 1 to 4 days, and MET and ProMET yeast strains were denoted. The supernatant was collected after culturing, and the yeast cells were lysed. Next, peptide fusion of the his-tag expression levels following TCA precipitation was detected through Western blotting. The housekeeping gene *GAPDH* was used as the internal control, and the results are presented in Fig. 1B, C. Since MET has a low molecular weight of around 3 kDa and the marker cannot be separated properly below 14 kDa, the MET major band showed the position closely to 14 kDa. The MET yeast strain was not expressed on the first day, but its expression increased and continued from the second to the third day. The ProMET yeast strain did not initially exhibit expression on the first day, but the expression level increased and continued from the second to the fourth day. Due to time and cost considerations in expression, MET and ProMET yeast strains were cultured for 2 days, and supernatants were collected for protein purification.

## Purification

Due to their small size, current separation systems and methods could not directly recover peptides. Thus, the his-tag and TEV protease-recognized fragments were fused before the target gene to establish a subsequent purification process. MET and ProMET yeast strains were cultured and centrifuged to collect the supernatant for nickel ion column purification. During purification, the following fractions were collected: flow-through (FT), wash (W), and elution (E). The FT, W, and E fractions were then analyzed through SDS-PAGE (Fig. 2A, B) to observe target bands. FT and E fractions exhibited protein bands and were subjected to Western blotting analysis to determine the target peptide position at 14 kDa, as shown in Fig. 2.

After dialysis, samples were treated with TEV protease and passed through a nickel ion column to remove the his-tag and TEV protease-recognized fragments. Flow-through

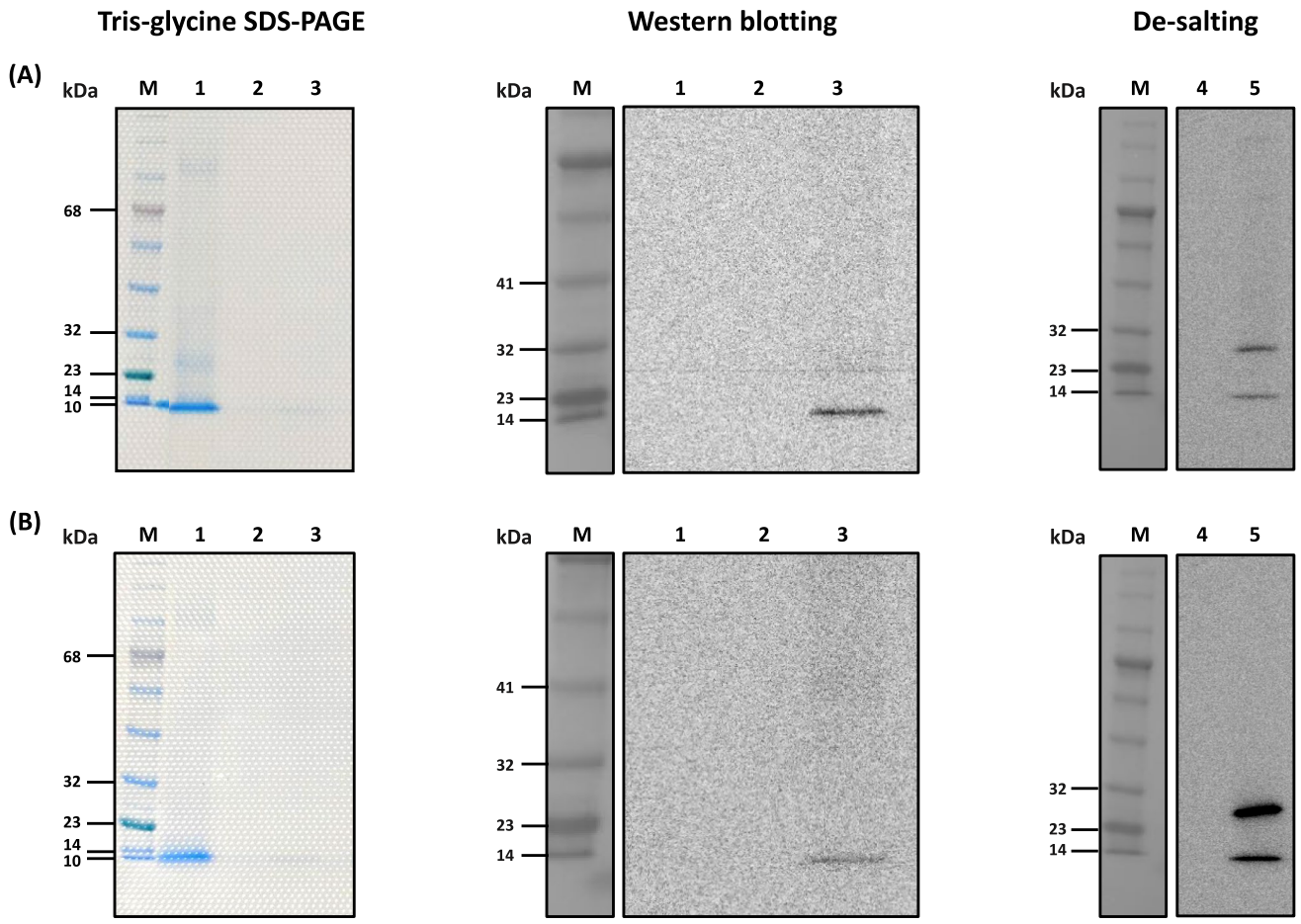


**Fig. 2** MET and ProMET purification analysis through histidine-affinity chromatography and desalting columns. **A** MET; **B** ProMET. Lane 1, flow-through; lane 2, wash; lane 3, elution; lane 4, desalting flow-through; lane 5, desalting elution

samples were collected for desalination in $ddH_2O$ as purified samples, and MET and ProMET were further analyzed through Western blotting. Two peptide bands were observed at 14 kDa and between 23 and 32 kDa in purified MET and ProMET samples, suggesting the oligomer formation (Fig. 2). Protein amounts were verified through Bradford; purified MET reached 1.68 µg/mL, and ProMET was 3.33 µg/mL.

## HPLC

The quality of purified MET and ProMET was analyzed through HPLC and compared with commercial (BV-CITEQ) and naturally extracted BV (BV-A4-1) (Fig. 3). BV-A4-1's main peak at a 1 mg/mL concentration was labeled Peak I. Given that melittin is the primary constituent of BV, Peak I serves as the qualitative marker for melittin, with a 23.123-min retention time and a 79.63% purity. Similarly, BV-CITEQ at 1 mg/mL exhibited a primary peak, Peak I, with a 23.599-min retention time and 85.02% purity. Peak II of BV-A4-1 and CITEQ corresponds to an unknown compound. The input protein concentration of MET purified in this study was 0.78 µg/mL, labeled Peak I, characterized by a 23.598-min retention time and 95.30% purity. Comparatively, ProMET had a 2.58 µg/mL input protein concentration, and Peak I indicated a 23.608-min retention time and 97.91% purity. Due to the larger protein molecule size from the fused MET with TEV cutting site, MET-no TEV was used as the non-protease treatment control. The major peak was Peak III, which exhibited a longer retention time of approximately 30 min.

## Mass spectrum

Amino acid sequences of purified MET and ProMET were analyzed using mass spectrometry. For MET, the sequence "GIGAV" was identified. With the MS/MS spectrum from the precursor ion (416.27 m/z, 1 +) (Fig. 4A), there were 2 b ions matched with the database (Fig. S3), confirming the existence of MET. For ProMET, the sequence "GAPEPEPAPEPEAEADAEADPEAGIGAVLK" was identified. Likewise, in the MS/MS spectrum from the precursor ion

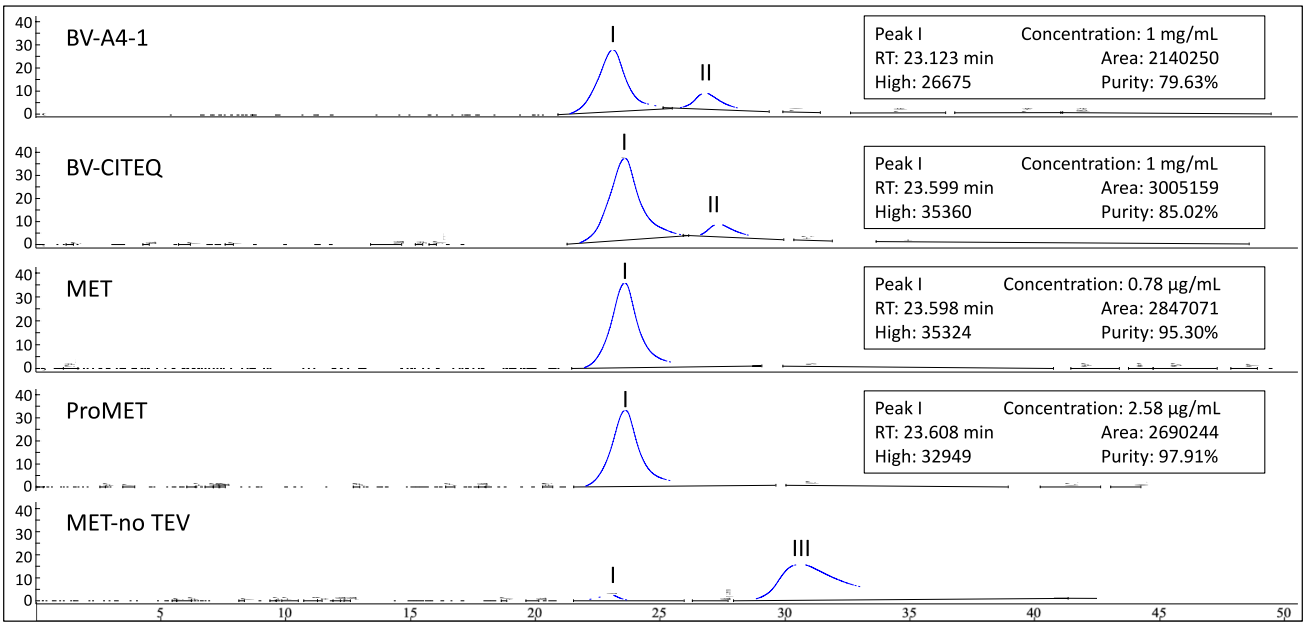


**Fig. 3** Identified peptide profiles of purified MET and ProMET compared with natural and commercial crude BV extract through HPLC. *BV-A4-1, natural crude BV extract; BV-CITEQ, commercial crude BV extract; MET, purified MET from this study; ProMET, purified ProMET from this study; MET-no TEV, TEV protease untreated MET. **Peak numbers: I, melittin or promelittin major peak; II, an unknown compound; III, non-protease treated MET constructed in this study

(976.45 m/z, 3 +) (Fig. 4B), there were 14 b ions and 18 y ions matched with the database (Fig. S4), confirming the existence of ProMET.

## NSC-34 cell regeneration tests

To understand melittin's effect on NSC-34 cell growth, we assessed cell proliferation ratios at 6, 12, and 24 h relative to 0 h. A standard NSC-34 cell-count curve was established in Fig. 5A. Cell counts in the BV-A4-1 and ProMET groups decreased 6 h post-treatment and significantly decreased at 12 and 24 h ($p > 0.05$), suggesting potential cytotoxicity. Treating the $H_2O$ and MET group exhibited no cytotoxicity at 6 h and significantly increased cell counts at 12 and 24 h compared to 0 h ($p < 0.05$) (Fig. 5B).

Following cellular damage induced by $H_2O_2$ stimulation, treating the MET group exhibited the highest cell regeneration ability between 12 and 48 h, followed by ProMET ($p < 0.05$). This result suggests that MET and ProMET, purified in this experiment, possess cell repair capabilities. BV-CITEQ and BV-A4-1 groups were comparable to those of the undamaged control group, indicating a certain repair effect (Fig. 6). The cell regeneration fold change (X) was highest in the MET and ProMET groups; 1.21- and 1.15-times higher than the undamaged control group after 12 h treatment, 1.19- and 1.09-times higher at 24 h, and 1.08- and 1.09-times higher at 48 h.

## Gene expression analysis of growth factors

MET effects on cell growth–related genes that promoted NSC-34 neuronal cell growth were evaluated. The results indicated that all treatment groups except ProMET stimulated cell growth–related factor expression compared to the control group (Fig. 7). Notably, the MET group exhibited a significant increase in *MAP2* expression ($p < 0.05$). *MAP2*, *MAPT*, *GAP-43*, *ChAT*, and *AChE* expressions in the treatment with BV-A4-1 and MET groups were upregulated compared to the control group, suggesting that these groups may promote cell growth.

# Discussion

Previously, purifying melittin from naturally extracted bee venom (BV) was a challenging task. While melittin is the primary component of BV, approximately 40–50% of its composition, achieving high purity through subsequent purification proved difficult due to various smaller molecular compounds and peptides (Gauldie et al. 1976). This study successfully expressed melittin (MET) and its precursor pro-melittin (ProMET) in the probiotic yeast *K. marxianus*. MET and ProMET were purified to yield 1.68 µg/mL and 3.33 µg/mL concentrations, respectively. Our proposed purification method utilized liquid chromatography results to compare the main separation peaks of

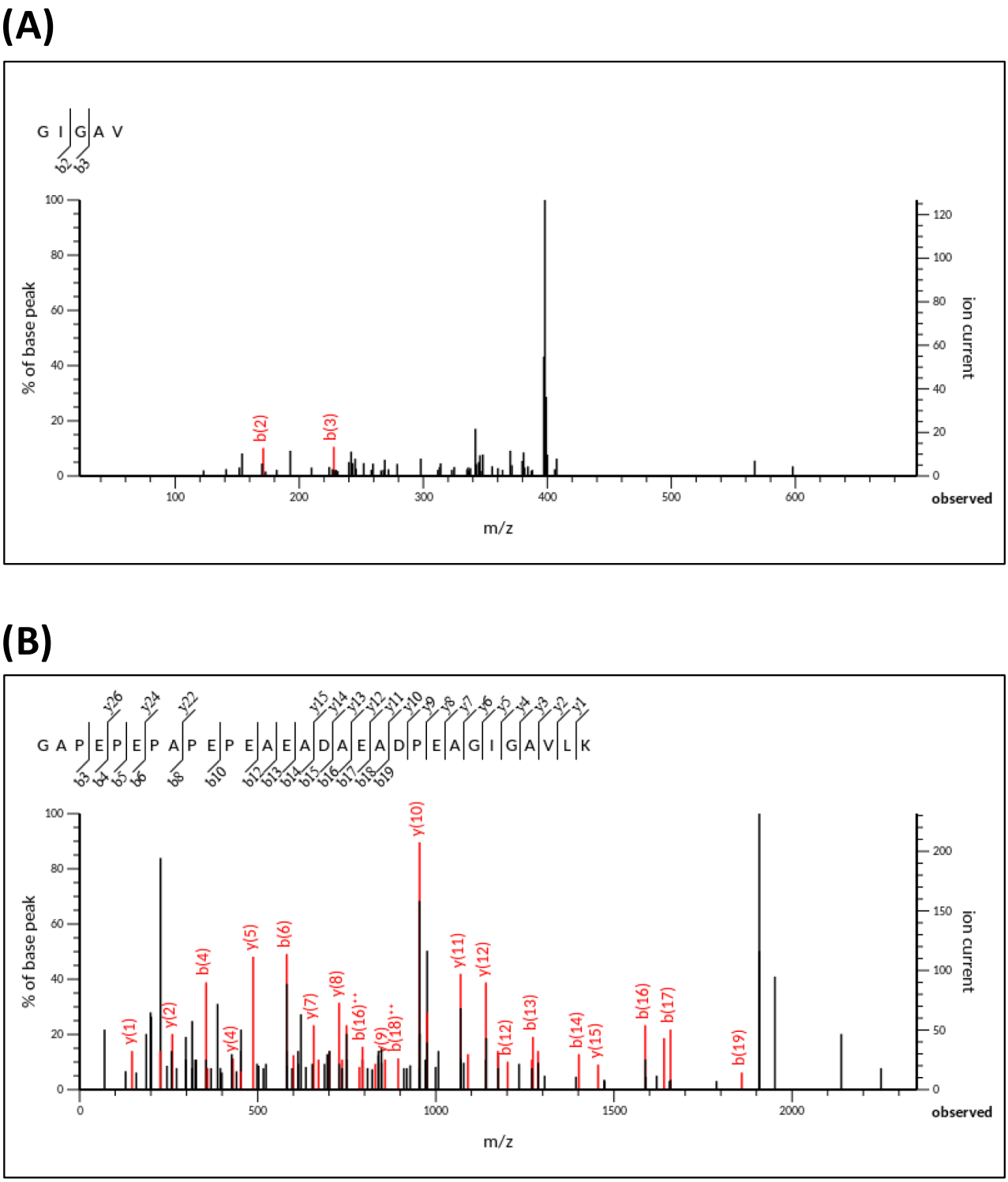


**Fig. 4** MS/MS spectrum of **A** MET and **B** ProMET sequences

melittin and pro-melittin produced by the major components found in BV. As a result, 95.30% MET and 97.91% ProMET purities were produced. These results are a notable improvement compared to commercially available purified melittin products, such as Sigma (M2272) with an 85% purity, Sigma (M7391) with a 65% purity, and Biosynth Carbosynth (XM176021) with a 70% purity.

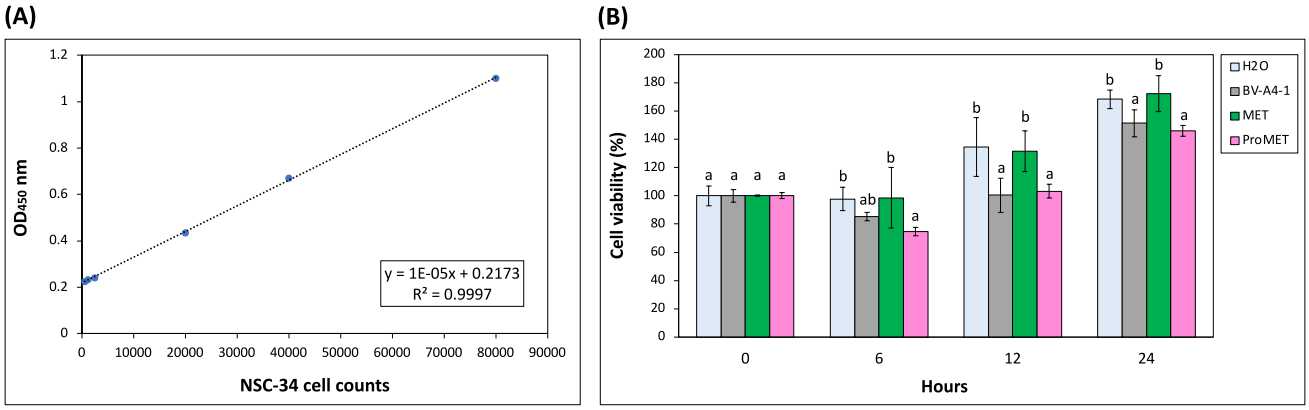


**Fig. 5** Safety assessment of purified MET and ProMET from treating NSC-34 neuron cells through the cell counting Kit-8. **A** Standard curve; **B** cell viability. *BV-A4-1, natural crude BV extract; MET, purified MET from this study; ProMET, purified ProMET from this study. **Values are averages of three replicated analyses with standard deviations. Significant differences ($p < 0.05$) between groups are indicated by the different letters above the bars

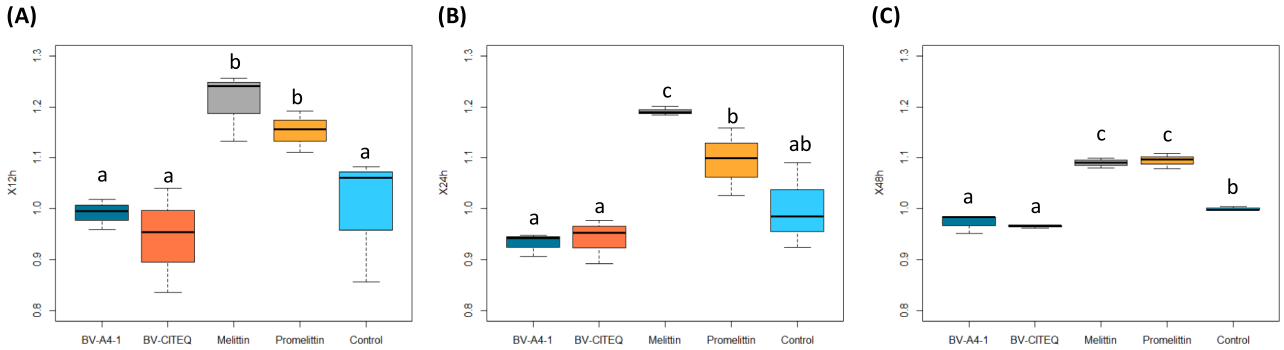


**Fig. 6** NSC-34 neuron cell regeneration fold change following $H_2O_2$ damage and treated with groups. **A** 12 h; **B** 24 h; **C** 48 h. *BV-A4-1, natural crude BV extract; BV-CITEQ, commercial crude BV extract; MET, purified MET from this study; ProMET, purified ProMET from this study; Control, non-$H_2O_2$-damaged control. **Values are averages of three replicated analyses with standard deviations. Significant differences ($p < 0.05$) between groups are indicated by the different letters above the bars

Currently, no product on the market matches the standard purity level achieved by the melittin purified in this study.

Naturally extracted BV and ProMET administration significantly reduced cell count, suggesting potential cytotoxicity. Furthermore, treatment at 12 and 24 h did not significantly increase cell growth. These results contrasted with the findings reported by Jung et al. (Jung et al. 2015), who found that naturally extracted BV substantially augmented cell growth compared to the control group. Although the BV employed in our experiment was crude, the unpurified BV composition ratio differed. The prominent active ingredient ratio remained distinct, making estimating the interactions between these substances challenging. In this study, MET displayed no cytotoxicity toward NSC-34 neuronal cells and significantly promoted NSC-34 cell growth. Therefore, our high-purity MET has significant application value for the purification process and finalized product.

During the NSC-34 cell regeneration test, NSC-34 cells enhanced regeneration from 12 to 48 h after MET treatment following $H_2O_2$ damage. In addition, we discovered that the BV and MET treatments upregulated *MAP2*, *MAPT*, and *GAP-43* gene expressions compared to the control group, especially the MET group. Corroborating the findings of Maier et al. (Maier et al. 2013), cell morphology and functional differentiation were regulated by cytoskeletal marker factor expressions, including *MAP2*, *MAPT*, and *GAP-43*, increasing during cell differentiation. Although there was no significant difference among *ChAT* expressions, there was still a slight improvement. The maturation of nerve cells is characterized by increased neuronal and cholinergic marker factor expressions, with *ChAT* as the primary enzyme responsible for catalyzing acetylcholine synthesis. Previous studies exploring Alzheimer's disease pathogenesis have revealed that *ChAT*

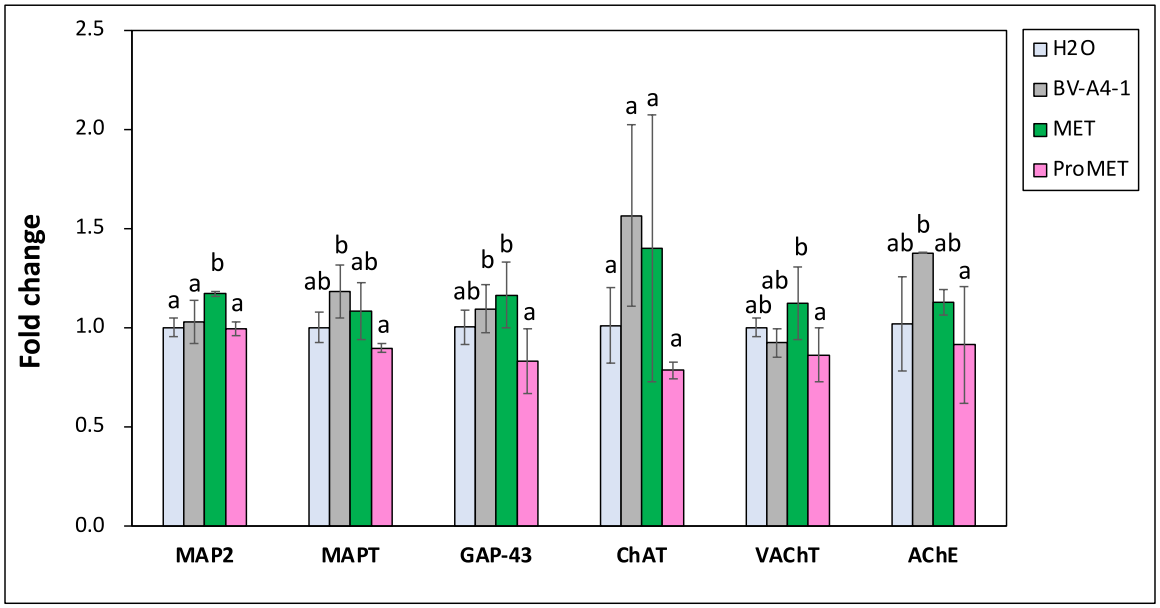


**Fig. 7** Gene expression analysis of growth factors in NSC-34 neuron cells treated with groups through qPCR. *BV-A4-1, natural crude BV extract; MET, purified MET from this study; ProMET, purified ProMET from this study. **Values are averages of three replicated analyses with standard deviations. Significant differences ($p < 0.05$) between groups are indicated by the different letters above the bars

expression is affected (Davies and Maloney 1976; Nagai et al. 1983; Ozturk et al. 2006; Perry et al. 1982). ChAT activity in the patient's cerebral cortex and hippocampus was significantly reduced, potentially determined by disease severity (Bierer et al. 1995). Our results indicated that *ChAT* expression in the BV and MET treatment groups was higher than in the control and ProMET groups, suggesting that BV and MET may enhance ChAT activity.

*ChAT* and *VAChT* genes share a common locus, the "cholinergic gene locus," and gene transcription regulatory elements (Eiden 1998). This genomic arrangement promoted the coordinated transcription regulation of both genes. By assuming the synergistic regulation of gene transcription, *VAChT* expression is expected to parallel *ChAT* expression, contradicting this experiment's results. Hollera et al. discovered that *VAChT* expression reached its maximum proliferation level in NSC-34 cells (Hollera et al. 1996). Typically, *AChE* expression in neurons precedes synaptogenesis, and increasing the *AChE* gene may serve as an effective biomarker for the endpoint maturation of NSC-34 cells (Maier et al. 2013). These findings indicate that MET enhances cell growth to maturity. Additional study is required to elucidate the underlying regulatory mechanisms. Taken together, we constructed a bionically manufactured melittin in probiotic yeast and evaluated its potential for promoting NSC-34 regeneration, paving the way for future commercial and pharmaceutical applications.

**Supplementary Information** The online version contains supplementary material available at https://doi.org/10.1007/s00253-024-13336-7.

**Acknowledgements** We thank Dr. Ming-Cheng Wu (Chung Hsing University, Department of Entomology) kindly provided natural crude BV extract. We are grateful to Dr. Pei-Chien Tsai (National Chung Hsing University, Department of Life Sciences) for assistance with NSC-34 cell culture experiments. We would like to thank the Wordvice for revising the manuscript.

**Author contribution** HY conducted experiments, analyzed the data, and prepared the drafted manuscript. HY contributed with scientific expertise in cell biology and funding acquisition. CY performed mass spectrum experiments, ML conducted protein purification experiments, CC provided scientific expertise in mass spectrometry, and RL supported the analytical work. YJ designed the project and finalized the manuscript preparation. All authors read and approved the final manuscript.

**Funding** This study was financially supported in part by the grant from Tungs' Taichung Metro-Harbor Hospital to Yu-Ju Lin (TTMHH-NCHULS111002, TTMHH-NCHULS112003, and TTMHH-NCHULS113003) and the National Science and Technology Council (NSTC 111–2313-B-005–037-, NSTC 112–2313-B-005–048-, and NSTC 113–2313-B-005–015-).

**Data availability** All data supporting the conclusions of this study are included in this published article (and its Supplementary files).

## Declarations

**Ethics approval and consent to participate** All authors read the manuscript and consent to the content.

**Consent for publication** All authors consented for publication.

**Competing interests** The authors declare no competing interests.



## References

Abd El-Wahed AA, Khalifa SA, Sheikh BY, Farag MA, Saeed A, Larik FA, Koca-Caliskan U, AlAjmi MF, Hassan M, Wahabi HA (2019) Bee venom composition: from chemistry to biological activity. Stud Nat Prod Chem 60:459–484. https://doi.org/10.1016/B978-0-444-64181-6.00013-9

Bierer LM, Haroutunian V, Gabriel S, Knott PJ, Carlin LS, Purohit DP, Perl DP, Schmeidler J, Kanof P, Davis KL (1995) Neurochemical correlates of dementia severity in Alzheimer's disease: relative importance of the cholinergic deficits. J Neurochem 64(2):749–760. https://doi.org/10.1046/j.1471-4159.1995.64020749.x

Carpena M, Nuñez-Estevez B, Soria-Lopez A, Simal-Gandara J (2020) Bee venom: an updating review of its bioactive molecules and its health applications. Nutrients 12(11):3360. https://doi.org/10.3390/nu12113360

Chen QC, Liu L, Yu TY, Tang L, Ml Y, Zhu WH, Jiang XY, Wang HY (2021) High-level expression and purification of melittin in *Escherichia coli* using SUMO fusion partner. Int J Pept Res Ther 27(1):9–15. https://doi.org/10.1007/s10989-020-10060-4

Davies P, Maloney A (1976) Selective loss of central cholinergic neurons in Alzheimer's disease. Lancet 308(8000):1403. https://doi.org/10.1016/S0140-6736(76)91936-X

Eiden LE (1998) The cholinergic gene locus. J Neurochem 70(6):2227–2240. https://doi.org/10.1046/j.1471-4159.1998.70062227.x

Fonseca GG, Heinzle E, Wittmann C, Gombert AK (2008) The yeast *Kluyveromyces marxianus* and its biotechnological potential. Appl Microbiol Biotechnol 79(3):339–354. https://doi.org/10.1007/s00253-008-1458-6

Gauldie J, Hanson JM, Rumjanek FD, Shipolini RA, Vernon CA (1976) The peptide components of bee venom. Eur J Biochem 61(2):369–376. https://doi.org/10.1111/j.1432-1033.1976.tb10030.x

Han SM, Kim JM, Park KK, Chang YC, Pak SC (2014) Neuroprotective effects of melittin on hydrogen peroxide-induced apoptotic cell death in neuroblastoma SH-SY5Y cells. BMC Complement Altern Med 14(1):286. https://doi.org/10.1186/1472-6882-14-286

Hollera T, Berse B, Cermak JM, Diebler M-F, Blusztajn JK (1996) Differences in the developmental expression of the vesicular acetylcholine transporter and choline acetyltransferase in the rat brain. Neurosci Lett 212(2):107–110. https://doi.org/10.1016/0304-3940(96)12808-1

Hong J, Wang Y, Kumagai H, Tamaki H (2007) Construction of thermotolerant yeast expressing thermostable cellulase genes. J Biotechnol 130(2):114–123. https://doi.org/10.1016/j.jbiotec.2007.03.008

Husseneder C, Donaldson JR, Foil LD (2016) Genetically engineered yeast expressing a lytic peptide from bee venom (Melittin) kills symbiotic Protozoa in the gut of Formosan subterranean termites. PLoS ONE 11(3):e0151675. https://doi.org/10.1371/journal.pone.0151675

Hwang DS, Kim SK, Bae H (2015) Therapeutic effects of bee venom on immunological and neurological diseases. Toxins 7:2413–2421. https://doi.org/10.3390/toxins7072413

Jung SY, Lee KW, Choi SM, Yang EJ (2015) Bee venom protects against rotenone-induced cell death in NSC34 motor neuron cells. Toxins 7(9):3715–3726. https://doi.org/10.3390/toxins7093715

Lee JE, Shah VK, Lee E-J, Oh M-S, Choi JJ (2019) Melittin – a bee venom component – enhances muscle regeneration factors expression in a mouse model of skeletal muscle contusion. J Pharm Sci 140(1):26–32. https://doi.org/10.1016/j.jphs.2019.03.009

Lee MH, Hsu TL, Lin JJ, Lin YJ, Kao YY, Chang JJ, Li WH (2020) Constructing a human complex type N-linked glycosylation pathway in *Kluyveromyces marxianus*. PLoS ONE 15(5):e0233492. https://doi.org/10.1371/journal.pone.0233492

Lee Y, Kim SG, Kim IS, Lee HD (2018) Standardization of the manufacturing process of bee venom pharmacopuncture containing melittin as the active ingredient. Evid Based Complement Alternat Med 2018:2353280. https://doi.org/10.1155/2018/2353280

Lin YJ, Chang JJ, Lin HY, Thia C, Kao YY, Huang CC, Li WH (2017) Metabolic engineering a yeast to produce astaxanthin. Bioresour Technol 245(Pt A):899–905. https://doi.org/10.1016/j.biortech.2017.07.116

Maier O, Böhm J, Dahm M, Brück S, Beyer C, Johann S (2013) Differentiated NSC-34 motoneuron-like cells as experimental model for cholinergic neurodegeneration. Neurochem Int 62(8):1029–1038. https://doi.org/10.1016/j.neuint.2013.03.008

Moon DO, Park SY, Lee KJ, Heo MS, Kim KC, Kim MO, Lee JD, Choi YH, Kim GY (2007) Bee venom and melittin reduce proinflammatory mediators in lipopolysaccharide-stimulated BV2 microglia. Int Immunopharmacol 7(8):1092–1101. https://doi.org/10.1016/j.intimp.2007.04.005

Moridi K, Hemmaty M, Akbari Eidgahi MR, Fathi Najafi M, Zare H, Ghazvini K, Neshani A (2020) Construction, cloning, and expression of melittin antimicrobial peptide using *Pichia pastoris* expression system. Gene Rep 21:100900. https://doi.org/10.1016/j.genrep.2020.100900

Muñoz A, López-García B, Marcos JF (2007) Comparative study of antimicrobial peptides to control citrus postharvest decay caused by *Penicillium digitatum*. J Agric Food Chem 55(20):8170–8176. https://doi.org/10.1021/jf0718143

Nagai T, McGeer P, Peng J, McGeer E, Dolman C (1983) Choline acetyltransferase immunohistochemistry in brains of Alzheimer's disease patients and controls. Neurosci Lett 36(2):195–199. https://doi.org/10.1016/0304-3940(83)90264-1

Ozturk A, DeKosky ST, Kamboh MI (2006) Genetic variation in the choline acetyltransferase (CHAT) gene may be associated with the risk of Alzheimer's disease. Neurobiol Aging 27(10):1440–1444. https://doi.org/10.1016/j.neurobiolaging.2005.08.024

Pacakova V, Štulík K, Hau PT, Jelinek I, Vinš I, Sýkora D (1995) Comparison of high-performance liquid chromatography and capillary electrophoresis for the determination of some bee venom components. J Chromatogr A 700(1–2):187–193. https://doi.org/10.1016/s0731-7085(00)00358-7

Perry R, Candy J, Perry E, Irving D, Blessed G, Fairbairn A (1982) Extensive loss of choline acetyltransferase activity is not reflected by neuronal loss in the nucleus of Meynert in Alzheimer's disease. Neurosci Lett 33(3):311–315. https://doi.org/10.1016/0304-3940(82)90391-3

Portell-Buj E, Vergara A, Alejo I, López-Gavín A, Monté MR, San Nicolás L, González-Martín J, Tudó G (2019) *In vitro* activity of 12 antimicrobial peptides against *Mycobacterium tuberculosis* and *Mycobacterium avium* clinical isolates. J Med Microbiol 68(2):211–215. https://doi.org/10.1099/jmm.0.000912

Pucca MB, Cerni FA, Oliveira IS, Jenkins TP, Argemí L, Sørensen CV, Ahmadi S, Barbosa JE, Laustsen AH (2019) Bee updated: current knowledge on bee venom and bee envenoming therapy. Front Immunol 10:2090. https://doi.org/10.3389/fimmu.2019.02090

Wang Y, Xiao J, Suzek TO, Zhang J, Wang J, Bryant SH (2009) PubChem: a public information system for analyzing bioactivities of small molecules. Nucleic Acids Res 37(Web Server issue):W623-33. https://doi.org/10.1093/nar/gkp456

Zhou L, Liu Z, Xu G, Li L, Xuan K, Xu Y, Zhang R (2020) Expression of melittin in fusion with GST in *Escherichia coli* and its purification as a pure peptide with good bacteriostatic efficacy. ACS Omega 5(16):9251–9258. https://doi.org/10.1021/acsomega.0c00085



## Authors and Affiliations

**Hsiao-Yun Huang[1] · Hung-Yi Hsu[2,3] · Cheng-Yu Kuo[4] · Mao-Lun Wu[1] · Chien-Chen Lai[4] · Gary Ro-Lin Chang[1] · Yu-Ju Lin[1]**

✉ Yu-Ju Lin
yjl@dragon.nchu.edu.tw

Hsiao-Yun Huang
hi4u2dws36@gmail.com

Hung-Yi Hsu
hungyihsu@gmail.com

Cheng-Yu Kuo
nini7702993@gmail.com

Mao-Lun Wu
mashmaroro661002@yahoo.com.tw

Chien-Chen Lai
lailai@dragon.nchu.edu.tw

Gary Ro-Lin Chang
gary590422@yahoo.com.tw

[1] Department of Life Sciences, National Chung Hsing University, No. 145, Xing-Da Road, South District, Taichung City 40227, Taiwan, ROC

[2] Section of Neurology, Department of Internal Medicine, Tungs' Taichung Metro-Harbor Hospital, No. 699, Section 8, Taiwan Boulevard, Wuqi District, Taichung City 43503, Taiwan, ROC

[3] Department of Post Baccalaureate Medicine, National Chung Hsing University, No.699, Section 8, Taiwan Boulevard, Wuqi District, Taichung City 43503, Taiwan, ROC

[4] Institute of Molecular Biology, National Chung Hsing University, No.145, Xing-Da Road, South District, Taichung City 40227, Taiwan, ROC